



# Internal cooling to produce aluminium alloy slurries for rheocasting

Yucel Birol\*

Materials Institute, Marmara Research Center, TUBITAK, Gebze, Kocaeli, Turkey

## ARTICLE INFO

### Article history:

Received 13 October 2008

Received in revised form 11 February 2009

Accepted 13 February 2009

Available online 4 March 2009

### Keywords:

Metals

Casting

Semi-solid processing

Rheocasting

## ABSTRACT

Rheocasting is becoming the choice of the casting industry which relies on the semi-solid processing for high integrity structural parts. It is thus of great technological interest to identify simple methods to prepare slurries at reduced cost. The potential of internal cooling to produce slurries for rheocasting was investigated in the present work for several aluminium casting alloys which are technologically important for aluminium foundries. Alloys quenched directly from the liquid state were predominantly dendritic while the slurry samples quenched after an initial fraction of solid phase was first formed, were dominated by  $\alpha$ -Al rosettes and globules. The solidification of the remaining liquid phase occurred through the growth of the  $\alpha$ -Al rosettes and globules which have formed during internal cooling before quenching.

© 2009 Elsevier B.V. All rights reserved.

## 1. Introduction

Reduced solidification shrinkage, shorter solidification time and laminar die filling offered in semi-solid metal casting, thanks to an already partially solid feedstock, give high integrity, heat treatable castings at die casting cycle times [1–3]. Of the two major routes employed in this high-volume, near-net shape manufacturing process, rheocasting is favored over thixocasting in recent years since the latter suffers from high cost of special non-dendritic feedstock and the inability to recycle its scrap. Molten alloy is treated into a slurry directly before casting in the rheocasting route [4], which thus tackles the cost issue and has become the choice of the casting industry which relies on semi-solid casting for high integrity structural parts [5,6].

While a number of rheocasting processes with attractive features have been proposed in recent years [7–10], the search for simple methods to prepare slurries at reduced cost is not over [11–13]. A new process, with a potential to meet such expectations was recently employed to produce A357 slurries for rheocasting [14]. This process relies on internal cooling of the melt into the semi-solid range to produce high quality slurries without an additional isothermal holding step before casting. It would be of great interest to apply this simple process to other Al casting alloys which are technologically important for aluminium foundries. The potential of internal cooling to produce slurries for rheocasting was investigated in the present work for several popular aluminium casting alloys with higher Si.

## 2. Experimental

The chemical compositions of the three alloys used in this study are given in Table 1. Alloy 1 is a general die casting alloy (AlSi8Cu3Fe) nearer to the eutectic composition with a relatively higher Si content than A357 alloy. Alloy 2 is a higher Si grade (AlSi10Mg) and is typically used for intricate, thin-walled castings that demand high strength while alloy 3 is a primary die casting alloy (Al9SiMgMn) widely used to manufacture automotive parts. The internal cooling process employed to produce slurries of these alloys is described in detail in [14] and is schematically illustrated in Fig. 1. The alloy ingot was melted in a carbon bonded silicon carbide crucible in an electric resistance furnace set at 700 °C. The melt thus obtained was then transferred to a second furnace set slightly above the liquidus point of the respective alloy. It was held in this furnace for at least 60 min to allow for temperature equilibration. The crucible was then withdrawn from the furnace and the melt was cooled internally, at approximately 1 °C s<sup>-1</sup>, by dissolving in it a pre-weighted solid block of the same alloy to achieve partial solidification. The solid block was attached to a stainless steel rod which was stirred at 1100 rpm until complete dissolution in the melt. The temperature of the melt and the weight of the solid alloy block were adjusted so as to achieve the desired solid fraction ( $F_s$ ) estimated from the  $F_s$  vs temperature ( $T$ ) curves (Table 2). The heat flow vs  $T$  data recorded during solidification at a scan rate of 2.5 °C min<sup>-1</sup> was used to obtain the  $F_s$  vs  $T$  curves to account for the rheo practice which relies on partial solidification of a molten alloy in contrast to the thixo practice which involves partial melting of a solid feedstock. The slurry thus obtained was sampled with a 2 cm<sup>3</sup> stainless steel cup and was immediately quenched in water. The water-quenched slurry samples were prepared with standard metallographic practices and were examined with an optical microscope.

## 3. Results and discussion

The heat flow vs  $T$  and  $F_s$  vs  $T$  curves of the three alloys investigated in the present work are shown in Fig. 2. The solidification exotherms reveal two neighbouring peaks, typical of hypo-eutectic Al–Si casting alloys (Fig. 2a). The smaller of the two peaks occurring at higher temperatures is linked with the primary solidification of the  $\alpha$ -Al matrix while the larger lower- $T$  peak is produced by

\* Tel.: +90 262 6773084; fax: +90 262 6412309.

E-mail address: [yucel.birol@mam.gov.tr](mailto:yucel.birol@mam.gov.tr).

**Table 1**  
Chemical composition of the aluminium casting alloys used in the present work (wt.%).

| Alloy | Si   | Fe    | Cu    | Mn    | Mg    | Ti    | Zn    | Sr    | Al   |
|-------|------|-------|-------|-------|-------|-------|-------|-------|------|
| 1     | 8.03 | 0.892 | 3.042 | 0.212 | 0.183 | 0.037 | 0.940 | 0.016 | Bal. |
| 2     | 9.85 | 0.131 | 0.072 | 0.011 | 0.312 | 0.156 | 0.020 | 0.004 | Bal. |
| 3     | 9.73 | 0.112 | 0.004 | 0.560 | 0.169 | 0.068 | 0.001 | 0.016 | Bal. |

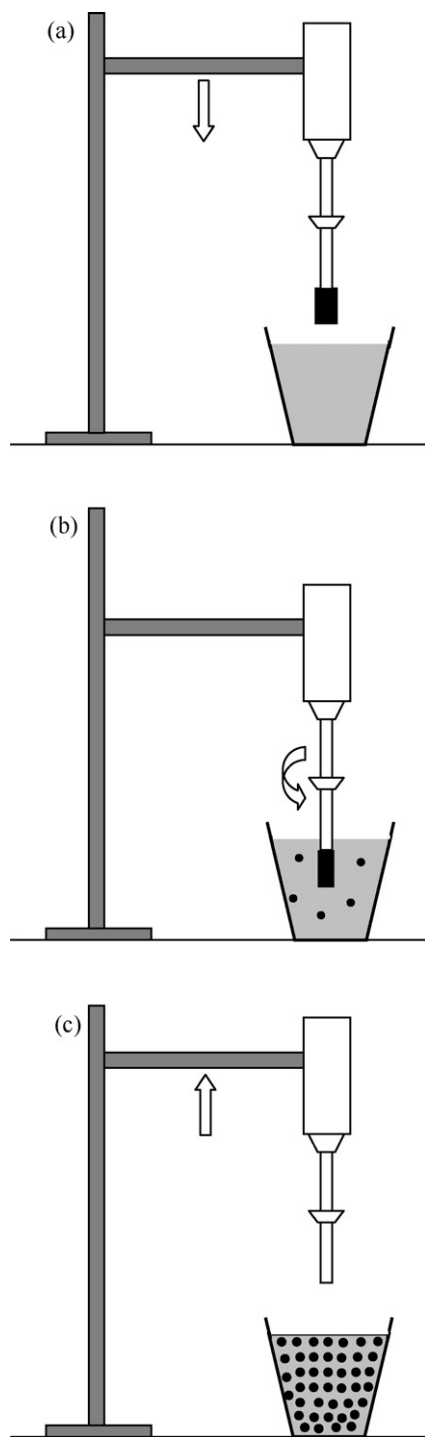


**Fig. 1.** Schematic illustration of the internal cooling practice employed in the present work: (a) solid block of the same alloy prepared in advance, attached to a stainless steel rod, (b) dissolved in the melt with simultaneous stirring action, and (c) the slurry thus produced.

the solidification of the Al–Si eutectic. The liquidus temperatures of alloys 1, 2 and 3 were identified from Fig. 1a to be 588 °C, 597 °C and 592 °C, respectively. The microstructures of the samples quenched from slightly above the liquidus points, from 600 °C, 610 °C and 605 °C for alloys 1, 2 and 3, respectively, are shown in Fig. 3. Fine  $\alpha$ -Al dendrites and the interdendritic eutectic phase, typical of hypoeutectic aluminium alloys, are readily identified in all alloys. The majority of the intermetallic particles were found by XRD and metallographic analysis to be  $\beta$ -Al<sub>5</sub>FeSi in alloys 1 and 2. The former additionally contained CuAl<sub>2</sub> particles.  $\alpha_c$ -Al<sub>12</sub>(Fe,Mn)<sub>3</sub>Si was the predominant intermetallic phase while several Al<sub>6</sub>(Fe,Mn) intermetallic particles were also noted in alloy 3. The  $\alpha$ -Al dendrites, the Al–Si eutectic and the intermetallic particles were all refined owing to the low-superheat casting conditions which prevailed in this first set of experiments. In spite of low-superheat casting conditions employed, these features are markedly different from those which have been shown to transform readily into globular structures upon reheating into the semi-solid temperature range in the thixo route [15–18], possibly due to the much higher solidification rates encountered in water quenching.

A second set of samples were produced by cooling the alloy melts into the semi-solid temperature range and then by quenching

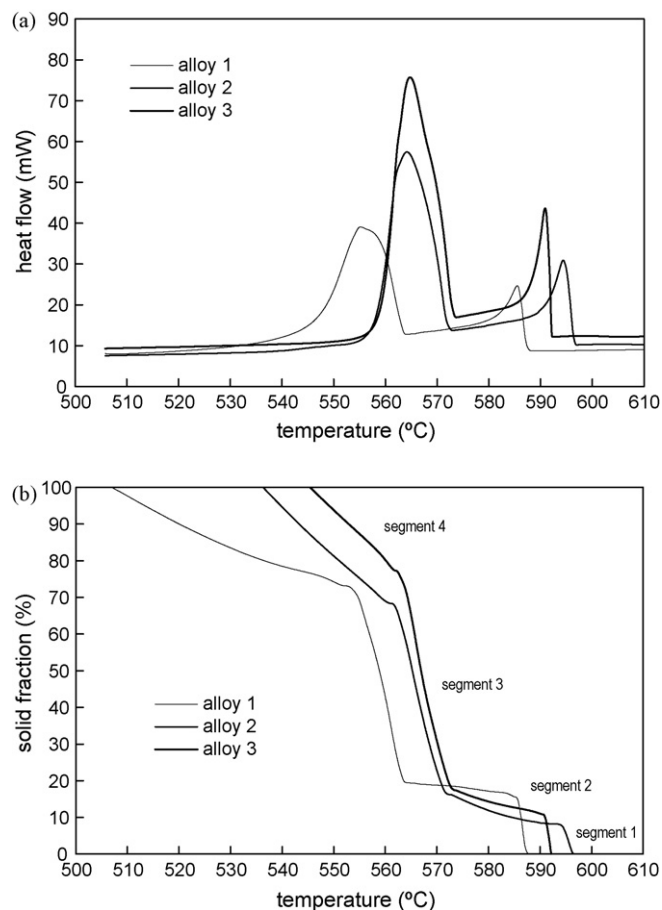


**Fig. 2.** (a) DSC and (b) solid fraction vs temperature curves of the three alloy obtained from heat flow vs temperature data recorded during cooling from the molten state.



**Table 2**

Parameters of the internal cooling process employed to produce slurries of the aluminium alloys listed in Table 1.

| Alloy | Weight (g)   |             | Temperature of the liquid alloy (°C) |       |
|-------|--------------|-------------|--------------------------------------|-------|
|       | Liquid alloy | Solid block | Initial                              | Final |
| 1     | 1275         | 77          | 604                                  | 571   |
| 2     | 1250         | 75          | 620                                  | 586   |
| 3     | 1366         | 79          | 620                                  | 587   |

the slurries thus obtained in water. The cooling rate in all experiments was nearly the same. Temperature of the slurry at the time of quenching dictates the solid fraction of the slurry which should be as high as possible to take full advantage of rheocasting without impairing its die filling ability. These temperatures were determined from the  $F_s$  vs  $T$  curves which typically reveal 4 segments with very similar features (Fig. 2b). The first and third segments

which start with the onset of primary and eutectic solidification, respectively, are nearly vertical and imply great sensitivity of the solid fraction to minor  $T$  fluctuations. The second and fourth segments are associated with the final stages of primary and eutectic solidification, respectively, and imply a relatively more gradual change in  $F_s$  with  $T$ . The former is nearly horizontal while the latter reveals an increasing slope from alloy 1 to alloy 3, with increasing Si content. It is clear from Fig. 2b that the last segment of the solidification interval is not at all appropriate due to the apparent difficulty involved in rheocasting slurries with a solid fraction over 70%. The first and third segments are not ideal either since the  $F_s$  changes substantially with very small temperature fluctuations inside this range, by nearly 8% for every degree change in  $T$  ( $0.08\text{ }^\circ\text{C}^{-1}$ ). The second segment of the solidification interval in each alloy, on the other

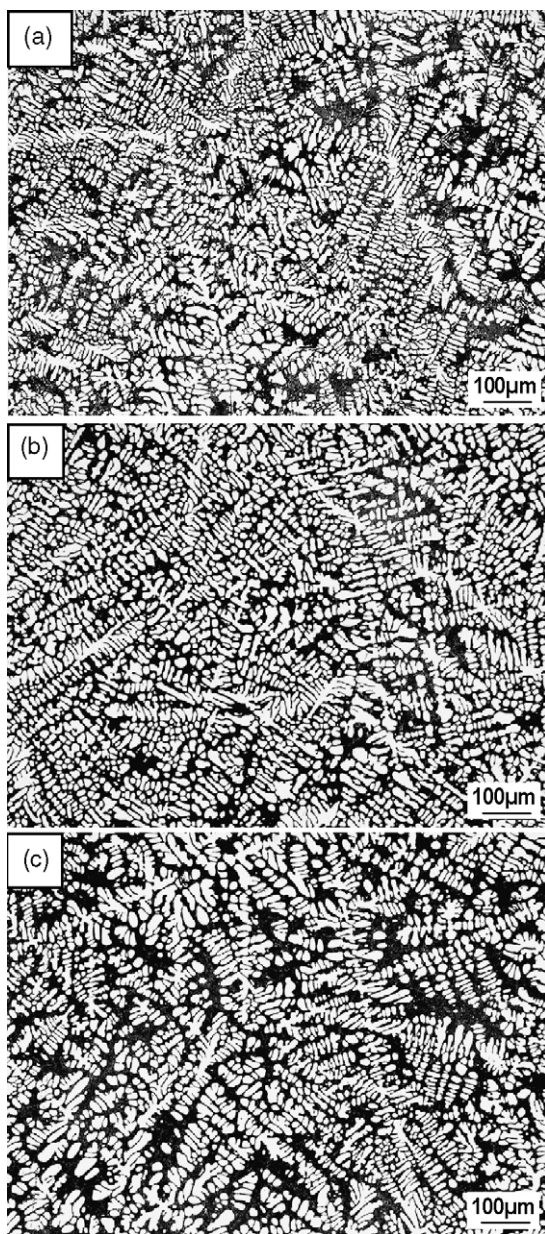


**Fig. 3.** Microstructures of alloy samples quenched from just above the liquidus point: (a) alloy 1 quenched from 600 °C, (b) alloy 2 quenched from 610 °C, and (c) alloy 3 quenched from 605 °C.

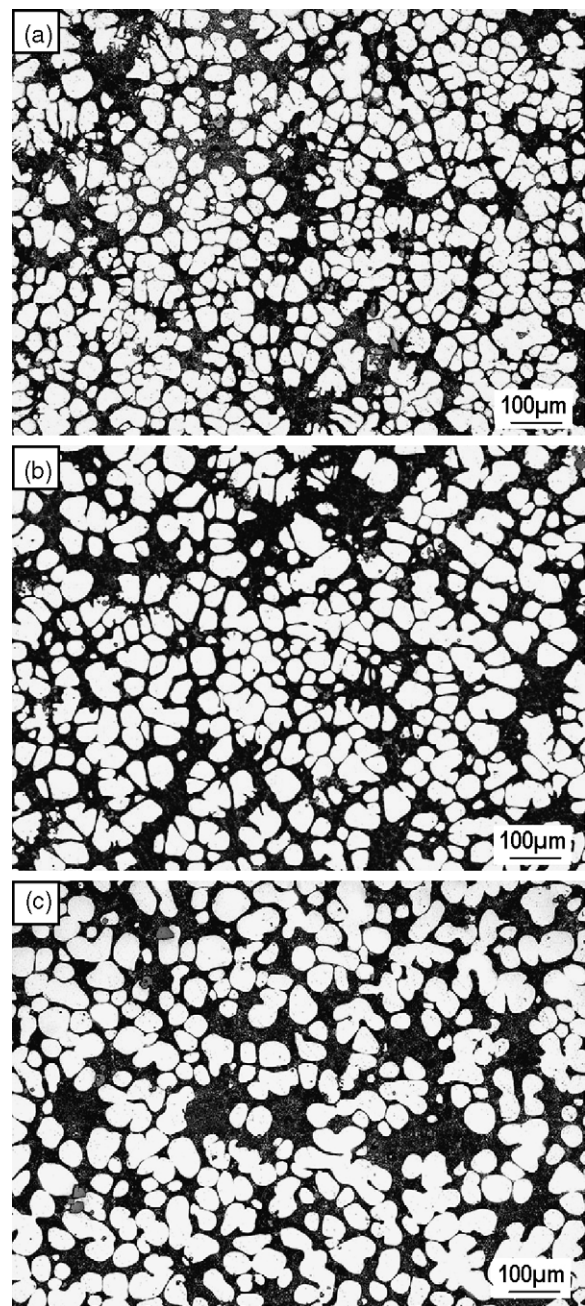


**Fig. 4.** Microstructures of slurry samples quenched from below the liquidus points: (a) alloy 1 quenched from 571 °C, (b) alloy 2 quenched from 586 °C, and (c) alloy 3 quenched from 587 °C.

hand, appears to be perfect in this regard.  $F_s$  is relatively independent of  $T$  in this range, i.e. large variations in  $T$  produce very small changes in  $F_s$ , only as much as  $0.002\text{ }^\circ\text{C}^{-1}$  for alloy 1. This segment spreads between  $563\text{ }^\circ\text{C}$  and  $586\text{ }^\circ\text{C}$ ,  $572\text{ }^\circ\text{C}$  and  $594\text{ }^\circ\text{C}$  and  $573\text{ }^\circ\text{C}$  and  $591\text{ }^\circ\text{C}$  for alloys 1, 2 and 3, respectively. Hence, melts were internally cooled into these temperature ranges, corresponding to solid fractions between 10 and 20% approximately and then were quenched in water.

Microstructural features of the quenched alloys changed substantially when they were first cooled internally into the liquid–solid phase field (Fig. 4). The slurry samples quenched after an initial fraction of solid phase (between 10 and 20%) is first formed, reveal no evidence of dendritic solidification. Instead, these samples are dominated by  $\alpha$ -Al rosettes and globules.  $\alpha$ -Al phase is believed to have nucleated continuously and uniformly throughout the entire volume of the melt during internal cooling with a small undercooling. The stirring action produced uniform temperature and solute fields around the primary  $\alpha$ -Al particles and similar growth rates in all directions via reducing constitutional undercooling. Stirring is thus instrumental in allowing the slurry to cool uniformly, promoting bulk nucleation. The hot ceramic mould also helped to maintain a uniform temperature field inside the melt by minimizing heat loss due to radiation. Dendritic growth was thus avoided and the primary particles readily became globular with time. The impact of nucleation throughout the melt and of forced convection on the primary solidification features confirms earlier reports [10,13]. It is fair to claim that the  $\alpha$ -Al nuclei forming throughout the entire volume of the melt promote a globular microstructure.

Considering that dendritic primary phase normally dominates at high cooling rates such as those encountered in water quenching, the non-dendritic morphology in the water-quenched slurry samples seems to imply that dendritic solidification is almost completely suppressed once a certain level of initial-primary solidification is achieved. The solidification of the remaining liquid phase apparently occurred through the growth of the  $\alpha$ -Al rosettes and globules which have formed during internal cooling before quenching. The final microstructure is a predominantly globular one. Such features, together with the adequate flowability achieved at these rather low solid fractions, are expected to provide a trouble-free rheocasting operation for the present alloys.

#### 4. Summary

Alloys quenched directly from the liquid state are predominantly dendritic while the slurry samples quenched after 10–20% solidification, are dominated by  $\alpha$ -Al rosettes and globules.  $\alpha$ -Al phase is believed to have nucleated uniformly throughout the entire volume of the melt during internal cooling. The stirring action produced uniform temperature and solute fields around the primary  $\alpha$ -Al particles and similar growth rates in all directions via reducing constitutional undercooling and thus promoted bulk nucleation. The solidification of the remaining liquid phase apparently occurred through the growth of the  $\alpha$ -Al rosettes and globules which have formed during internal cooling before quenching and have become globular with time.

#### Acknowledgements

It is a pleasure to thank Mr. O. Çakır and Mr. F. Alageyik for their help with the experiments and the State Planning Organization of Turkey for the financial support.

#### References

- [1] M.C. Flemings, *Met. Trans. A* 22A (1991) 957.
- [2] D.H. Kirkwood, *Inter. Mater. Rev.* 39 (1994) 173.
- [3] Z. Fan, *Inter. Mater. Rev.* 47 (2002) 49.
- [4] J.A. Yurko, R.A. Martinez, M.C. Flemings, SAE World Congress, Detroit, Michigan, March 3–6, 2003, 2003-01-0433.
- [5] J. Yurko, M. Flemings, A. Martinez, *Die Casting Engineer* 48 (2004) 50.
- [6] D. Apelian, Q.Y. Pan, M. Findon, *Die Casting Engineer* 48 (2004) 22.
- [7] P.J. Uggowitzer, H. Kaufmann, *Steel Res. Int.* 75 (2004) 525.
- [8] M.C. Flemings, R.A. Martinez-Ayers, M.A. de Figueredo, J.A. Yurko Metal alloy compositions and process, US Patent 6,645,323 B2 (2003).
- [9] D. Dautre, J. Langlais, S. Roy, in: D. Apelian, A. Alexandrou (Eds.), *Proceedings of the 8th International Conference on Semi-solid Processing of Alloys and Composites*, Limassol, Cyprus, 2004, pp. 397–408.
- [10] Z. Fan, X. Fang, S. Ji, *Mater. Sci. Eng. A* 412 (2005) 298.
- [11] J. Wannasin, R.A. Martinez, M.C. Flemings, *Scripta Mater.* 55 (2006) 115.
- [12] S.K. Kim, Y.Y. Yoon, H.H. Jo, *J. Mater. Process. Technol.* 187 (2007) 354.
- [13] C.P. Hong, J.M. Kim, *Solid State Phenomena* 116–117 (2006) 44.
- [14] Y. Birol, *J. Alloys Compds.*, submitted for publication.
- [15] Y. Birol, *J. Alloys Compd.*, doi:10.1016/j.jallcom.2008.02.093.
- [16] Y. Birol, *J. Alloys Compd.*, doi:10.1016/j.jallcom.2008.05.074.
- [17] Y. Birol, *Int. J. Mater. Res.* 98 (2007) 1019.
- [18] Y. Birol, *J. Mater. Sci.* 43 (2008) 3577.